

# Relationship Between DNA Damage Response, Initiated by Camptothecin or Oxidative Stress, and DNA Replication, Analyzed by Quantitative 3D Image Analysis

K. Berniak,<sup>1</sup> P. Rybak,<sup>1</sup> T. Bernas,<sup>1,2</sup> M. Zarębski,<sup>1</sup> E. Biela,<sup>1</sup> H. Zhao,<sup>3</sup> Z. Darzynkiewicz,<sup>3</sup> J. W. Dobrucki<sup>1\*</sup>

<sup>1</sup>Division of Cell Biophysics, Faculty of Biochemistry, Biophysics and Biotechnology, Jagiellonian University, Krakow, Poland

<sup>2</sup>Nencki Institute of Experimental Biology, Laboratory of Functional and Structural Tissue Imaging, Polish Academy of Sciences, Warsaw, Poland

<sup>3</sup>Brander Cancer Research Institute, Department of Pathology, New York Medical College, Valhalla, New York 10595

Received 21 January 2013; Revision Received 29 May 2013; Accepted 6 June 2013

Grant sponsor: NCN; Grant numbers: UMO-2011/01/B/NZ3/00609, 2012/05/E/ST2/02180; Grant sponsor: EU Structural Funds; Grant number: BMZ No. POIG.02.01.00-12-064/08; Grant sponsor: NCI; Grant number: CA R01 28 704; Grant sponsor: R.A. Welke Cancer Research Foundation.

This article is an expanded version of the communication, which was delivered during 2012 ISAC Congress in Leipzig.

K. Berniak and P. Rybak contributed equally to this work.

\*Correspondence to: J. W. Dobrucki, Division of Cell Biophysics, Faculty of Biochemistry, Biophysics and Biotechnology, Jagiellonian University, Krakow, Poland. E-mail: jerzy.dobrucki@uj.edu.pl

Published online in Wiley Online Library (wileyonlinelibrary.com)

DOI: 10.1002/cyto.22327

© 2013 International Society for Advancement of Cytometry

- A method of quantitative analysis of spatial (3D) relationship between discrete nuclear events detected by confocal microscopy is described and applied in analysis of a dependence between sites of DNA damage signaling ( $\gamma$ H2AX foci) and DNA replication (EdU incorporation) in cells subjected to treatments with camptothecin (Cpt) or hydrogen peroxide ( $H_2O_2$ ). Cpt induces  $\gamma$ H2AX foci, likely reporting formation of DNA double-strand breaks (DSBs), almost exclusively at sites of DNA replication. This finding is consistent with the known mechanism of induction of DSBs by DNA topoisomerase I (topo1) inhibitors at the sites of collisions of the moving replication forks with topo1-DNA “cleavable complexes” stabilized by Cpt. Whereas an increased level of H2AX histone phosphorylation is seen in S-phase of cells subjected to  $H_2O_2$ , only a minor proportion of  $\gamma$ H2AX foci coincide with DNA replication sites. Thus, the increased level of H2AX phosphorylation induced by  $H_2O_2$  is not a direct consequence of formation of DNA lesions at the sites of moving DNA replication forks. These data suggest that oxidative stress induced by  $H_2O_2$  and formation of the primary  $H_2O_2$ -induced lesions (8-oxo-7,8-dihydroguanosine) inhibits replication globally and triggers formation of  $\gamma$ H2AX at various distances from replication forks. Quantitative analysis of a frequency of DNA replication sites and  $\gamma$ H2AX foci suggests also that stalling of replicating forks by Cpt leads to activation of new DNA replication origins. © 2013 International Society for Advancement of Cytometry

## Key terms

DNA damage; DNA damage response; DDR;  $\gamma$ H2AX; histone H2AX phosphorylation; DNA replication; camptothecin; oxidative stress; hydrogen peroxide; cell cycle; base excision repair

It has been demonstrated that a relationship between DNA damage response (DDR, also defined as DNA damage signaling) and DNA replication can be studied and quantitatively analyzed within a population of adherent cells in vitro, using laser scanning cytometry (LSC). Cell measurements by LSC, combined with multivariate data analysis, made it possible to correlate the drug-induced DNA damage response in individual cells with a specific phase of the cell cycle, inhibition of replication, an increased level of a specific protein, or induction of apoptosis (1–9). However, LSC analysis can neither provide information on the relationship between these processes in time and in space within the same nucleus, nor can it reveal whether DNA damage response occurs within or outside the sites of DNA replication (“replication factories”). When DNA damage signaling occurs at the sites of DNA replication, it is likely that the damage is causally related to movement of DNA replication forks. It is also possible to envisage a different scenario, where these two events coincide in time, but not in space, i.e., the DNA damage signaling occurs during S-phase, but is induced away from replication forks because the two events are not causally related.

Thus, in order to discern between these two scenarios, in addition to LSC analysis, spatial patterns of DDR and replication foci need to be investigated in 3D by microscopy.

To extend our prior findings linking induction of DDR and DNA replication (5,9), in this study, we used 3D fluorescence confocal microscopy and image analysis to reveal spatial relationship between DDR and DNA replication. The DNA damage signaling inflicted by the DNA topoisomerase I inhibitor camptothecin (Cpt) or hydrogen peroxide ( $H_2O_2$ ) was used as a test case to validate and optimize a method of quantitative image analysis dedicated to investigating spatial relationships between DNA replication sites and DDR foci.

It is known that Cpt induces DDR, revealed as phosphorylation of histone H2AX on Ser139 (induction of  $\gamma$ H2AX foci) and activation of ATM (Ataxia telangiectasia mutated kinase), exclusively in cells replicating DNA (8–10). In the case of oxidative DNA damage inflicted by  $H_2O_2$ , the induction of  $\gamma$ H2AX foci was apparent in both, DNA replicating as well as not replicating cells. The level of  $\gamma$ H2AX expression, however, was significantly higher in S-phase cells (Fig. 1). On the other hand, it was uncertain to what extent the sites representing DNA damage signaling, namely  $\gamma$ H2AX foci, known to mark primarily the presence of DNA double-strand breaks [(DSBs; (12,13)], were spatially associated with the DNA replication sites in S-phase cells exposed to  $H_2O_2$ .

In this report, we describe a method of quantitative analysis of a spatial relationship between  $\gamma$ H2AX foci and DNA replication sites, the latter detected by labeling newly synthesized (nascent) DNA with EdU (5-ethynyl-2'-deoxyuridine) and “click chemistry” (7,14), in cells exposed to Cpt or  $H_2O_2$ . Our analysis of a spatial association between these foci in 3D images of A549 human lung adenocarcinoma cell nuclei confirms that Cpt induces  $\gamma$ H2AX foci almost exclusively in association with DNA replication sites. In contrast, although the frequency of  $H_2O_2$ -induced  $\gamma$ H2AX foci is distinctly elevated in S-phase cells, they are located predominantly outside of sites of DNA replication.

## MATERIALS AND METHODS

### Cell Cultures

In vitro cultures of human lung adenocarcinoma A549 intended for imaging experiments were grown on round coverslips submerged in Petri dishes, as described previously (6,15).

### Inducing DNA Damage by Cpt or $H_2O_2$ and Labeling Nascent DNA

DNA precursor analog, EdU (10  $\mu$ M, Click-iT<sup>®</sup> EdU AlexaFluor<sup>®</sup> 488 Imaging Kit cat. # C10337; Invitrogen/Molecular Probes) was added to cell cultures 30 min before adding Cpt or  $H_2O_2$ . Cpt or  $H_2O_2$  was added to culture medium at a final concentration of 0.2  $\mu$ M or 0.2 mM, respectively. After 30 min of exposure to a drug (i.e., 60 min of exposure to EdU), cells were fixed. Untreated cells were incubated with EdU for 60 min. Detection of EdU was performed according to manufacturer's instructions. In control experiments, we demonstrated that EdU, at a concentration and

exposure time we used, induced no detectable increase of the level of phosphorylation of histone H2AX, indicating that no DDR was evoked by the precursor (data not shown).

### Detection of $\gamma$ H2AX

Cells were fixed with methanol-free formaldehyde (4%, EMS, Hatfield, PA) and treated with Triton X-100 (0.1%, Sigma, Poznań, Poland). Blocking was done overnight in 3% (w/v) BSA (Sigma, Poznań). Phospho-specific (Ser139)  $\gamma$ H2AX mAb (Upstate Biotechnology, Lake Placid, NY) was used, followed by a secondary antibody AlexaFluor<sup>®</sup> 568 goat anti-mouse IgG (H+L), cat. # A11004 (Invitrogen/Molecular Probes).

### Laser Scanning Cytometry

LSC experiments were performed as described previously (5–7).

### Confocal Microscopy

Images of cell nuclei with fluorescently labeled EdU and  $\gamma$ H2AX were recorded using Leica LSC SP5 confocal microscope (Leica Microsystems GmbH, Wetzlar, Germany). The following instrumental parameters were used: 63 $\times$  HCX PL APO CS NA 1.4 oil immersion lens, excitation 488 (Ar) and 561 nm (HeNe), emission detection bands 500–550 nm for AlexaFluor488 (Click-iT EdU), and 600–660 nm for AlexaFluor568 (immunofluorescence,  $\gamma$ H2AX), registration in sequential mode, scanning 8000 Hz (resonant scanner), with 8–16 frames averaged.

### Image Processing and Analysis

3D images of DNA replication and histone phosphorylation were deconvolved using AutoDeblur software v.X2.2 (Media Cybernetics, Rockville, MD). The area occupied by the nucleus was selected and the histogram of fluorescence intensities was edited to remove noise and background. The images of DNA replication (EdU) sites had negligible background, whereas the immunofluorescence images of  $\gamma$ H2AX foci always resulted in a low but detectable level of nonspecific signal, which had to be carefully estimated and removed by histogram editing. The 3D object counter plugin (16) for Image J was used to determine the position and the number of 3D objects in a stack. The coordinates of the centers of mass (barycenters) of each focus were calculated. This procedure was repeated for both fluorescence channels (replication and histone phosphorylation). A script written in Python was used to measure the distances from a selected  $\gamma$ H2AX focus to all EdU sites. The set of all distances from all  $\gamma$ H2AX foci to their nearest EdU site were used to construct a histogram of the distances to the nearest-neighbor. This procedure was repeated for each nucleus.

## RESULTS

### Quantitative Analysis of Distances Between $\gamma$ H2AX Foci and DNA Replication (EdU) Sites

Our previous attempt to quantify the spatial relationship between DNA replication sites and  $\gamma$ H2AX foci by means of colocalization analysis, based on 2D images, yielded results that gave only an approximate indication of the existence of

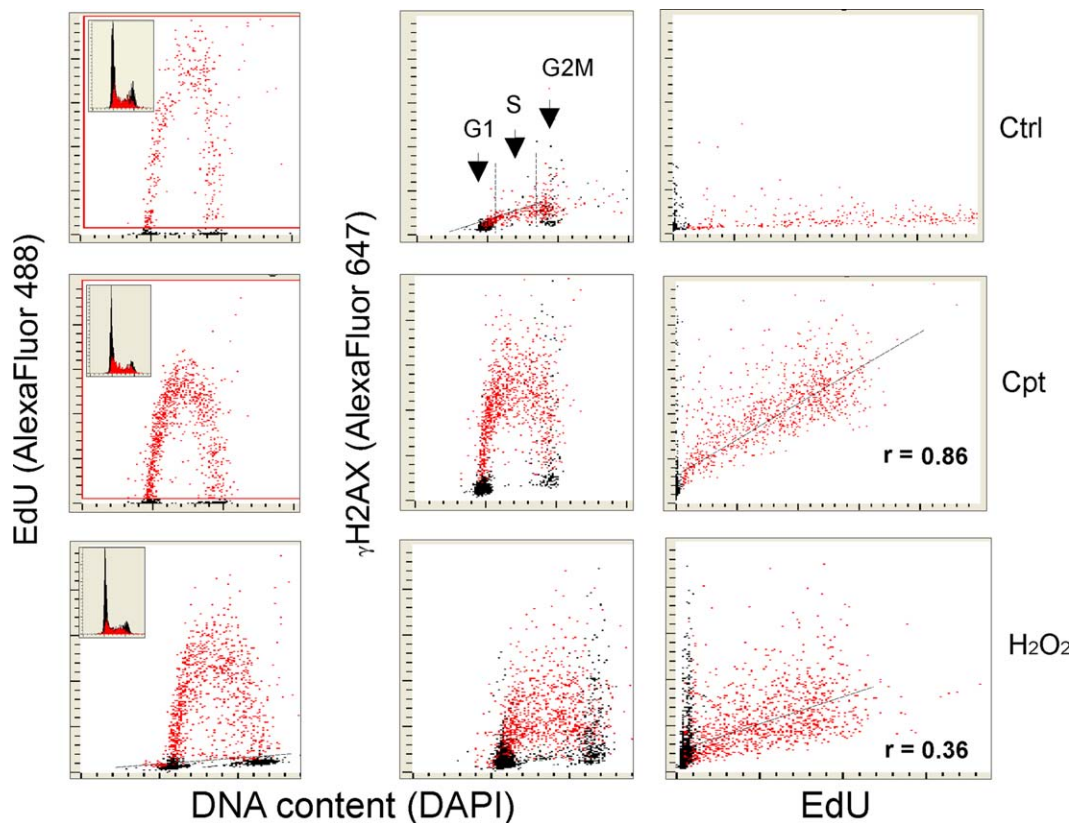


**Figure 1.** Relationship between DNA replication and induction of  $\gamma$ H2AX in A549 cells treated with Cpt or  $\text{H}_2\text{O}_2$ ; analysis by laser scanning cytometry (LSC; data from (6,8)). Exponentially growing A549 cells were exposed only to  $20\ \mu\text{M}$  EdU for 2.5 h (top panels), exposed to EdU for 30 min and then (still in the presence of EdU) treated either with  $0.2\ \mu\text{M}$  Cpt for 2 h (mid panels), or exposed to EdU and then treated with  $200\ \mu\text{M}$   $\text{H}_2\text{O}_2$  (bottom panels). The cells that incorporated EdU were “paint-gated” (red dots) and the data were plotted as bivariate distributions representing  $\gamma$ H2AX versus DNA content (mid-columns), or  $\gamma$ H2AX versus EdU incorporation (center and right columns). Note that Cpt induced  $\gamma$ H2AX only in EdU incorporating cells; this is consistent with a known mechanism of action of the DNA-bound Cpt causing collapse of replication forks (11). However, in response to treatment with  $\text{H}_2\text{O}_2$ , although  $\gamma$ H2AX was still preferentially induced in S-phase cells, it was also induced in some cells not-replicating DNA (black dots; G<sub>1</sub> and G<sub>2</sub>M) cells. A correlation between EdU incorporation and induction of  $\gamma$ H2AX was much stronger in cells treated with Cpt ( $r = 0.86$ ) than with  $\text{H}_2\text{O}_2$  ( $r = 0.36$ ). Insets in the left row panels present DNA content frequency histograms from the respective cultures. While the LSC data show the relationship between DNA replication versus induction of  $\gamma$ H2AX at the level of individual cells they do not reveal whether the damage signaling occurs in replicating areas. Cell imaging studies are needed to observe a relationship between the induction of  $\gamma$ H2AX foci and actual DNA replication in particular local sections of DNA within the nucleus. [Color figure can be viewed in the online issue which is available at [wileyonlinelibrary.com](http://wileyonlinelibrary.com).]

spatial dependence between the two events (6,8). In these prior estimates, correlation coefficients depended on the areas (or volumes) of the differentially labeled replication versus phosphorylation regions. However, it is not the area of the overlap of these sites, but the spatial proximity between them in 3D space that has to be used as a criterion to distinguish whether the damage signaling is induced within the replicating or nonreplicating DNA regions. In this study, therefore, for the purpose of analysis of interdependencies between  $\gamma$ H2AX foci and replication sites, we measured the distances between the centers of mass (barycenters) of  $\gamma$ H2AX foci and the nearest DNA replication regions. Representative images (Fig. 2) and analyses of distances between barycenters of EdU sites and  $\gamma$ H2AX foci in untreated cells as well as cells exposed to Cpt or  $\text{H}_2\text{O}_2$  (over 350 nuclei) are shown in Figures 3–5; the numerical data are summarized in Tables 1 and 2.

In untreated cells, there was a very low level of histone H2AX phosphorylation in nonreplicating cells (Figs. 1 and 2)

( $\sim 11$  phosphorylation foci/nucleus; Table 2), and a higher number in EdU-labeled cells ( $\sim 25$ – $30$ /nucleus). This is consistent with the previous data reporting lower level of constitutive DNA damage signaling in G<sub>1</sub>- compared with S-phase cells (1,4,5). Because the pattern of DNA replication is distinctly different in early-, mid-, and late S-phase (8,18) (Fig. 2), these stages were analyzed separately.

The histograms of distances in 3D space between the  $\gamma$ H2AX foci and the nearest DNA replication regions in Cpt-treated cells demonstrate that a large proportion of  $\gamma$ H2AX foci are located close (less than  $0.5\ \mu\text{m}$ ) to the sites of replicating DNA (Figs. 4A, 4D, and 4G). It should be noted that these histograms embrace Cpt-induced as well as endogenous phosphorylation foci, the latter reporting constitutive DNA damage signaling induced primarily by endogenous oxidants (1–3). However, in untreated cells, very few phosphorylation foci were found within  $0.5\ \mu\text{m}$  of the nearest replication site (Figs. 3A, 3C, and 3E).

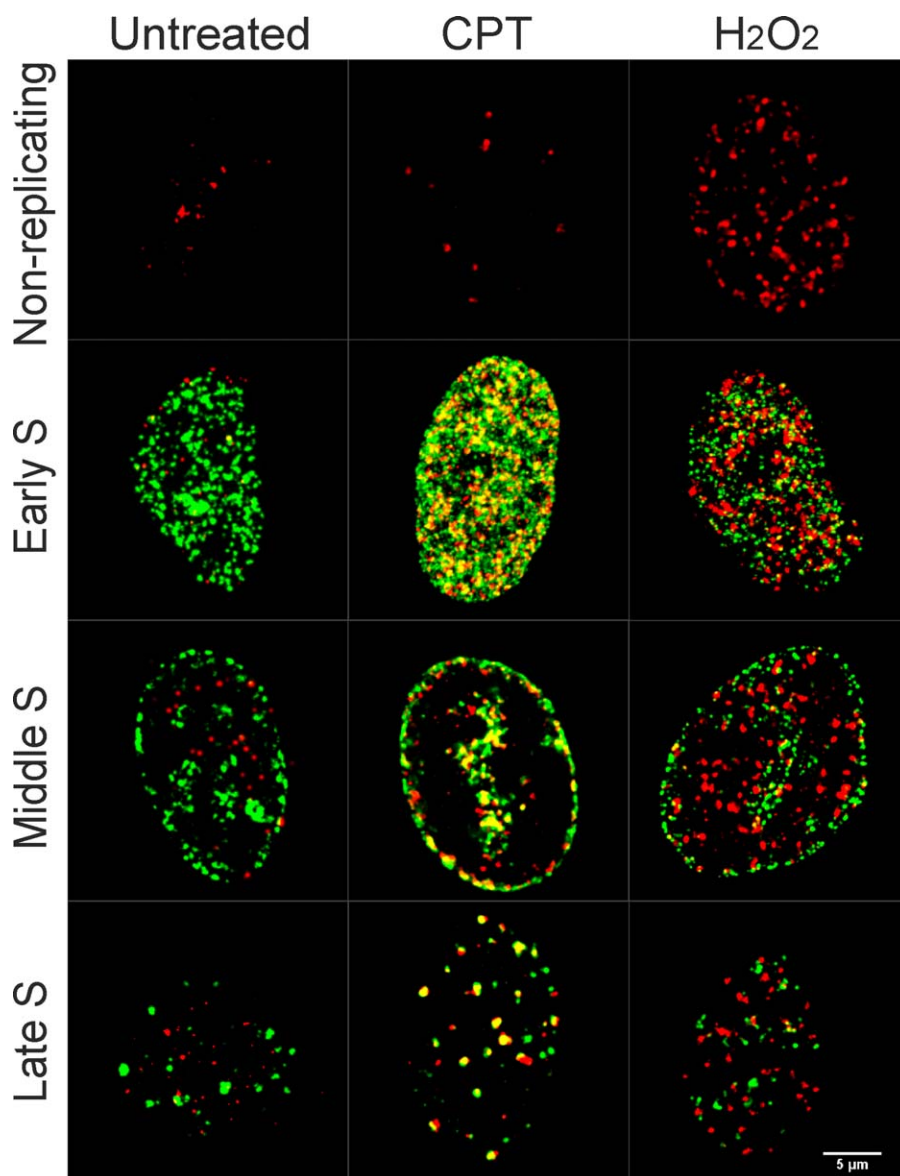


**Figure 2.** Representative images of  $\gamma$ H2AX foci (red) and replication regions (green) in nuclei of nonreplicating and replicating cells (early, mid, and late S-phase), untreated or treated with Cpt or  $H_2O_2$ . An equatorial region of each nucleus is shown (maximum projection of 10 confocal planes).

The shape of the histograms representing untreated cells differs significantly between the subsequent S-phase sub-stages. Clearly, the three stages of S-phase pose different problems for analysis of distances between  $\gamma$ H2AX and EdU sites. It is noticeable that the number of replication foci (Table 1) and the ranges of the measured distances are different in the three morphologically recognizable sub-stages of S-phase in untreated and Cpt-treated cells. The left side of each histogram (short distances) represents  $\gamma$ H2AX foci located within DNA replicating areas (Figs. 4A, 4D, and 4G). Likely, they represent DNA damage (DSBs) inflicted by Cpt at the site of DNA replication forks. The right side of the histogram represents  $\gamma$ H2AX foci located at a relatively large distance from the replication sites. The width of the histograms (which is defined by

replication-independent endogenous  $\gamma$ H2AX foci located far from replication) is larger in mid- and late- (Figs. 4D and 4G) than in early S-phase (Fig. 4A; Table 2).

In early S-phase of Cpt-treated cells, the DNA replication sites are very numerous ( $227 \pm 143$ /nucleus; Table 1); the median distance between the sites in 3D space is  $\sim 0.74 \mu\text{m}$  and the median distance between  $\gamma$ H2AX foci and the nearest DNA replication region is  $0.53 \mu\text{m}$ . Consequently, all  $\gamma$ H2AX foci, even the ones that may be unrelated to replication, are found quite near to some EdU incorporation sites. Mid-S sub-phase is characterized by an even larger number of DNA replication sites ( $276 \pm 89$ /nucleus). However, they are clustered primarily around nucleoli and under the nuclear envelope. They are separated by a median distance of  $0.77 \mu\text{m}$ . In late S-

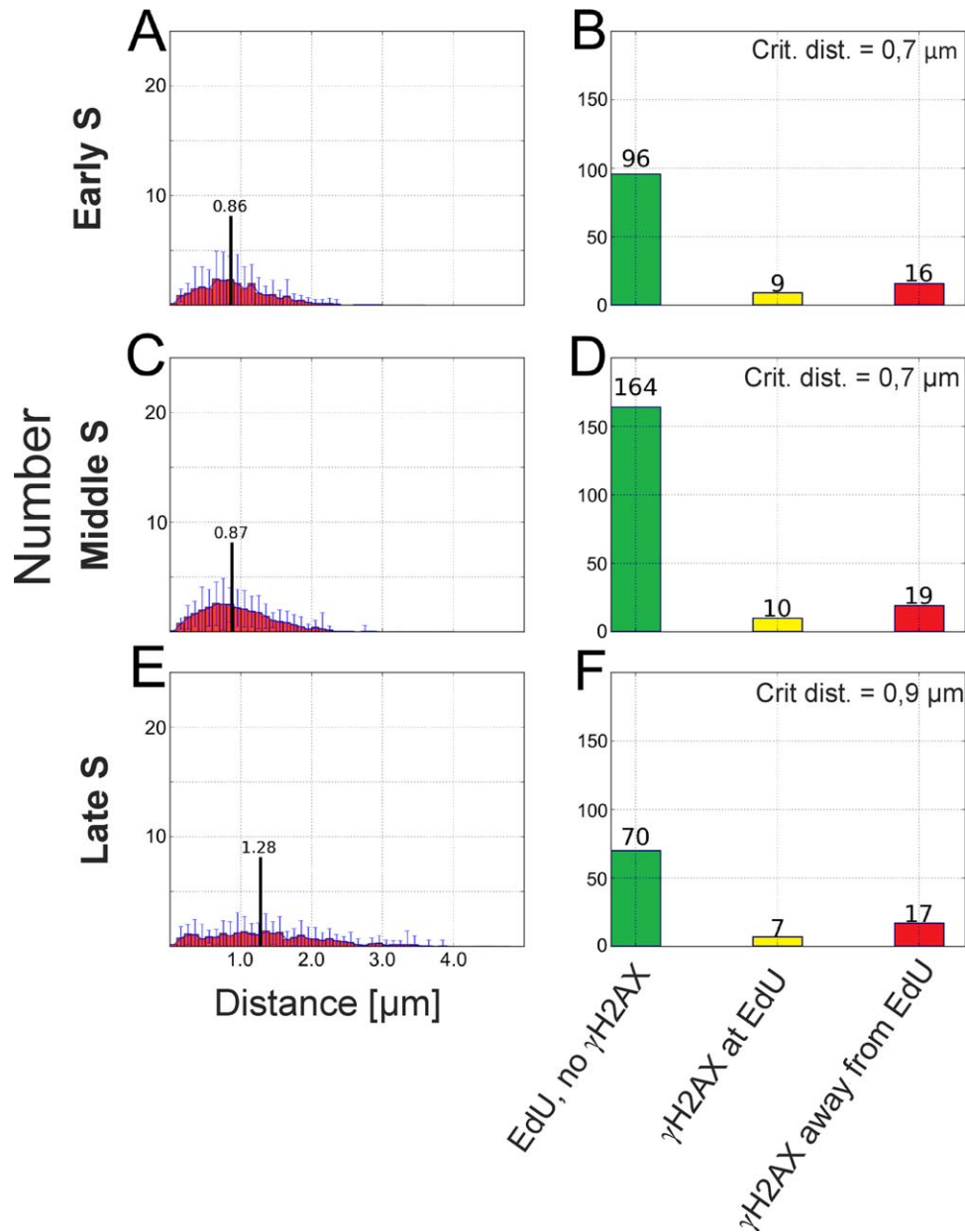


**Figure 3.** Analysis of distances from histone H2AX phosphorylation (endogenous DNA damage signaling) to replication foci in control, untreated cells. Left column—Histograms of  $\gamma$ H2AX-to-replication distances in cells in early, mid, and late S-phase; the median value is indicated. Right column—A bar graph representing the numbers of undamaged replication foci not accompanied by  $\gamma$ H2AX (left),  $\gamma$ H2AX foci adjacent to replication foci (center), and  $\gamma$ H2AX foci located outside of replicating regions (right). [Color figure can be viewed in the online issue which is available at [wileyonlinelibrary.com](http://wileyonlinelibrary.com).]

phase, in Cpt-treated cells, DNA replication is confined to relatively few ( $99 \pm 64$ /nucleus), well spaced areas (the median EdU-to-EdU sites distance is  $1.01 \mu\text{m}$ ); some  $\gamma$ H2AX foci are found even as far as  $4.51 \mu\text{m}$  from the nearest EdU-region. In other words, the histograms extending further into long distances for mid and late S-phase reflect the increasing average distances between DNA replicating regions in the course of progression through S-phase. Considering the above, the late S-phase cells are expected to have the lowest number of  $\gamma$ H2AX foci unrelated to replication that are, however, in prox-

imity to the replication regions. Consequently, this period appears to be the most suitable for assessing the spatial relationship between DNA damage signaling (histone H2AX phosphorylation) and DNA replication.

#### Correcting for Intrinsic (endogenous) $\gamma$ H2AX Foci Unrelated to Cpt and $\text{H}_2\text{O}_2$ Treatment

It is important to note that the histograms shown in Figures 4A, 4D, and 4G as well as 5A, 5D, and 5G embrace not only the lesions induced by Cpt or  $\text{H}_2\text{O}_2$ , but the intrinsic

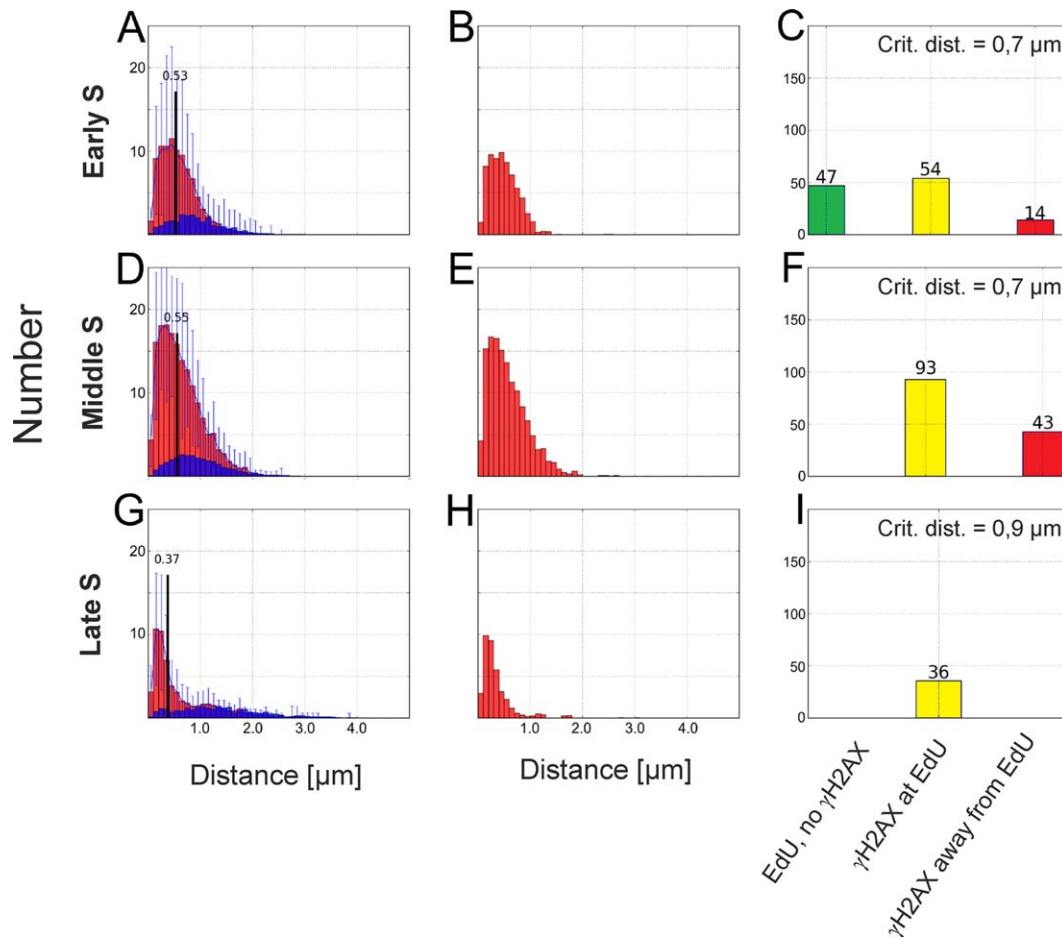


**Figure 4.** Analysis of distances from histone H2AX phosphorylation to replication foci in Cpt-treated cells. **A, D, G:** Histograms of  $\gamma$ H2AX-to-replication distances in cells in early, mid, and late S-phase; note that data include Cpt-induced and endogenous H2AX phosphorylation foci. The median value is indicated. **B, E, H:** Histograms of  $\gamma$ H2AX-to-replication distances in cells in early, mid, and late S-phase, after subtracting the histogram representing the endogenous phosphorylation foci (marked in blue). Similarity between histograms representing Cpt-treated cells and the corresponding control (untreated) cells was quantified with Kolmogorov-Smirnov and QF (17) metrics ( $\mu\text{m}$ ; parenthesis), yielding values of 0.42 (1.60), 0.33 (1.34), 0.69 (3.10) for early, mid, and late S, corresponding to 99% confidence limit, i.e., the difference between the histograms was statistically significant. **C, F, I:** A bar graph representing the numbers of undamaged replication foci, i.e., not accompanied by  $\gamma$ H2AX (left),  $\gamma$ H2AX foci adjacent to replication foci (center), and  $\gamma$ H2AX foci located outside of replicating regions (right). [Color figure can be viewed in the online issue which is available at [wileyonlinelibrary.com](http://wileyonlinelibrary.com).]

$\gamma$ H2AX foci as well. The intrinsic foci are present in untreated cells [Fig. 2 (top row) and Fig. 3] where, as mentioned, they report constitutive DNA damage signaling induced most likely by endogenous oxidants generated in mitochondria as by-products of aerobic respiration (1–3,6,19). Thus, the specific analysis of DNA damage signaling induced by Cpt or  $\text{H}_2\text{O}_2$  requires separating Cpt- and  $\text{H}_2\text{O}_2$ -induced foci from the intrinsic  $\gamma$ H2AX foci. This was achieved by subtracting the histograms representing control, untreated cells (i.e., the histograms shown in Fig. 3) from the histograms representing all  $\gamma$ H2AX foci in Cpt- or  $\text{H}_2\text{O}_2$ -treated cells (Fig. 4B, E, H and Fig. 5B, E, H). All the three corrected histograms representing Cpt-treated cells (Fig. 4B, E, H) are strongly asymmetric and show a majority of the  $\gamma$ H2AX foci located within no more than  $1\mu\text{m}$  of the nearest replication site. This result was expected because Cpt is known to cause DSBs at the sites of moving replication forks (11). The histograms representing

the  $\text{H}_2\text{O}_2$  treatment do not show such asymmetry, revealing that histone  $\gamma$ H2AX foci do not cluster in close proximity of DNA replication sites (Fig. 5B, E, H). This issue is discussed further in the text. The precise assessment of the numbers of DSBs (or  $\gamma$ H2AX foci) occurring in and outside of replication areas as a result of both treatments requires analysis of the distances separating  $\gamma$ H2AX foci from the nearest replication sites, as described below.

#### Counting DNA Replication-Dependent $\gamma$ H2AX Foci

The goal of this work is to quantitatively analyze a relationship between the induction of  $\gamma$ H2AX foci and DNA replication (Edu sites). Toward this end, it is necessary to measure frequency (the actual number) of replication-dependent and independent  $\gamma$ H2AX foci. This quantitative analysis hinges upon a correct criterion for distinguishing the dependent (neighboring) from independent (located afar)

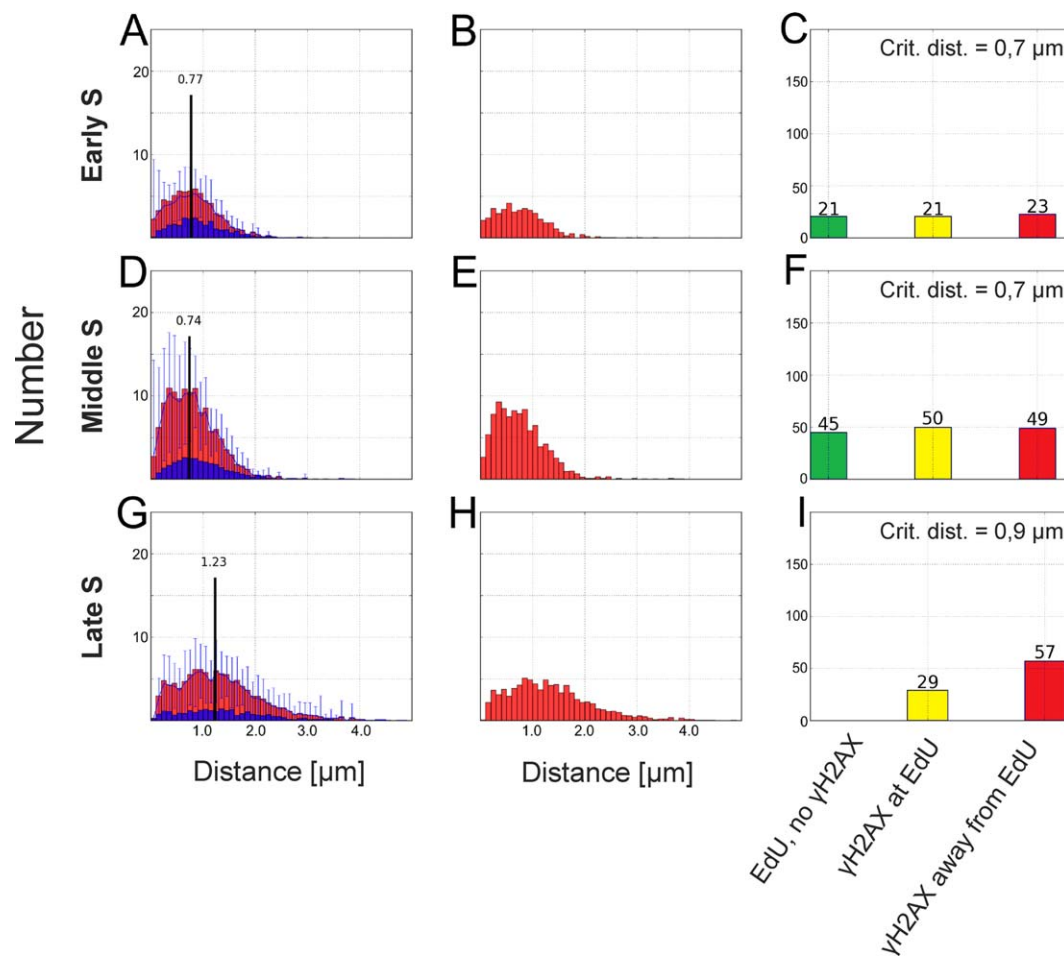


**Figure 5.** Analysis of distances from histone H2AX phosphorylation to replication foci in  $\text{H}_2\text{O}_2$ -treated cells. **A, D, G:** Histograms of  $\gamma\text{H2AX}$ -to-replication distances in cells in early, mid, and late S-phase; note that data include  $\text{H}_2\text{O}_2$ -induced and endogenous histone phosphorylation foci. The median value is indicated. **B, E, H:** Histograms of  $\gamma\text{H2AX}$ -to-replication distances in cells in early, mid, and late S-phase, after subtracting the histogram representing the endogenous phosphorylation foci (marked in blue). Similarity between histograms representing  $\text{H}_2\text{O}_2$ -treated cells and the corresponding control (untreated) cells was quantified with Kolmogorov-Smirnov and QF (17) metrics ( $\mu\text{m}$ ; parenthesis), yielding values of 0.15 (0.58), 0.15 (0.67), 0.05 (0.20) for early, mid, and late S, indicating no statistically significant difference. Analysis of similarity between the data representing Cpt- and  $\text{H}_2\text{O}_2$ -treated cells yielded the values of 0.30 (1.05), 0.18 (0.68), and 0.7 (3.02), indicating a statistically significant differences for early and late S (95% confidence limit), but not for mid-S, where the number of replication foci was the highest. **C, F, I:** A bar graph representing the numbers of undamaged replication foci, i.e., not accompanied by  $\gamma\text{H2AX}$  (left),  $\gamma\text{H2AX}$  foci adjacent to replication foci (center), and  $\gamma\text{H2AX}$  foci located outside of replicating regions (right). [Color figure can be viewed in the online issue which is available at [wileyonlinelibrary.com](http://wileyonlinelibrary.com).]

events. Such distinction has to rely on the knowledge of distances between the barycenters of the  $\gamma\text{H2AX}$  and EdU labeled sites. A question arises as to what distance between the barycenters is to be expected when H2AX phosphorylation occurs within a replicating area—in its center or at the periphery. The barycenters of the dependent events (i.e., damage signaling induced in a replicating area) are not expected to coincide ideally in 3D space for the following reasons: (i) in the protocol, the EdU labeling pulse of the replication sites was of 30 min duration. A large area of nascent DNA was, therefore, labeled exclusively on one side of the DSB created by Cpt, before replication forks encountered Cpt-stabilized DNA-topoisomerase I (topo1) complexes terminating their progression (Fig. 6). H2AX phosphorylation occurred during the span of 30 min after the initial exposure to Cpt or  $\text{H}_2\text{O}_2$  along

megabase domain of DNA on both flanks of the DSB (Fig. 6) along hundreds of nucleosomes (13,20); (ii) some contribution to a separation between the barycenters of the labeled nascent DNA and histone phosphorylation regions may also come from chromatin unfolding, relaxation, and movements that occur following the damage (21).

In addition to the above, the nascent DNA (EdU labeled) and chromatin with phosphorylated H2AX regions are, to some degree, misrepresented by optical microscopy (Fig. 6). Specifically, the size of images of very small foci exceeds their actual physical size in as much as even the smallest labeled regions are represented by an ellipsoid of  $\sim 250$ – $500$  nm in diameter and at least  $700$  nm in length. Thus, the H2AX phosphorylation that occurred in the replication focus, and the replication area itself, are represented by relatively large,

**Table 1.** Summary of numerical data extracted from analyses of all replication foci in untreated, and Cpt and H<sub>2</sub>O<sub>2</sub>-treated cells.

		REPLICATION FOCI			
		NON. REPL.	EARLY S	MIDDLE S	LATE S
Total number/cell	Control		107 ± 56	175 ± 36	79 ± 43
	Cpt		227 ± 143*	276 ± 89*	99 ± 64
	H <sub>2</sub> O <sub>2</sub>		155 ± 66*	285 ± 166*	93 ± 45
Foci volume (median) [ $\mu\text{m}^3$ ]	Control		0.0365	0.0515	0.0877
	Cpt		0.0248	0.0267	0.0510
	H <sub>2</sub> O <sub>2</sub>		0.0201	0.0379	0.0847
Repl. to repl. distance (median; max) [ $\mu\text{m}$ ]	Control		0.9; 3.76	0.95; 2.82	1.22; 5.24
	Cpt		0.74; 2.85	0.77; 2.92	1.01; 5.9
	H <sub>2</sub> O <sub>2</sub>		0.83; 2.46	0.77; 2.88	1.10; 5.05
Percent of all replication foci, accompanied by $\gamma\text{H2AX}$ signal	Control		9.87%	6.47%	7.33%
	Cpt		36.61%*	44.65%*	45.28%*
	H <sub>2</sub> O <sub>2</sub>		24.29%*	26.55%*	27.81%*

The data pertinent to the number of replication foci, and the percentage of replication foci that are accompanied by  $\gamma\text{H2AX}$  signal were analyzed by the Student's test; the values that are statistically different from control (95% confidence limit) are marked with asterisk.

possibly overdrawn, regions of fluorescence. In summary, even in the case, where the damage is inflicted at a particular replication fork, the barycenters of both labeled regions ( $\gamma\text{H2AX}$  and replication) can eventually be separated by a measurable distance at a time when the cell is fixed. The knowledge about this particular distance is of importance for distinguishing replication-dependent and independent damage events.

This maximum distance between the centers of images representing regions of H2AX phosphorylation and damaged

DNA replication area is a sum of four values: (i) the average radius of a replication region (in early and mid-S phase, approximately 400 nm and 600 nm in late S), (ii) the distance between the barycenters of replication and histone phosphorylation which arises from the fact that phosphorylation occurs on both sides of replication, whereas nascent DNA is located only on one side of the DNA break, we assume this to reach ~100 nm, (iii) the error in measuring the position of each barycenter which may reach ~100 nm in our system,

**Table 2.** Summary of numerical data extracted from analyses of all  $\gamma\text{H2AX}$  foci in untreated, and Cpt and H<sub>2</sub>O<sub>2</sub>-treated cells.

		HISTONE PHOSPHORYLATION FOCI ( $\gamma\text{H2AX}$ )			
		NON. REPL.	EARLY S	MIDDLE S	LATE S
Total number /cell	Control	11 ± 18	26 ± 20	30 ± 16	25 ± 15
	Cpt	8 ± 7	94 ± 68*	166 ± 66*	60 ± 27*
	H <sub>2</sub> O <sub>2</sub>	83 ± 31	70 ± 17*	129 ± 33*	112 ± 26*
Foci volume (median) [ $\mu\text{m}^3$ ]	Control	0.0505	0.0393	0.0503	0.0449
	Cpt	0.0803	0.0627	0.0562	0.0856
	H <sub>2</sub> O <sub>2</sub>	0.0459	0.0548	0.1278	0.1605
$\gamma\text{H2AX}$ to $\gamma\text{H2AX}$ distance (median, max) [ $\mu\text{m}$ ]	Control	1.79; 15.97	1.35; 10.62	1.57; 6.43	1.65; 7.44
	Cpt	2.33; 14.72	1.03; 6.54	0.99; 4.4	1.39; 5.41
	H <sub>2</sub> O <sub>2</sub>	1.07; 3.14	1.18; 4.34	1.17; 3.78	1.24; 5.16
$\gamma\text{H2AX}$ to repl. distance (median, max) [ $\mu\text{m}$ ]	Control		0.86; 3.57	0.87; 3.98	1.28; 4.76
	Cpt		0.53; 2.91	0.55; 3.43	0.37; 4.51
	H <sub>2</sub> O <sub>2</sub>		0.77; 3.32	0.74; 3.89	1.23; 6.07
Percent of all $\gamma\text{H2AX}$ foci associated with replication, minus control (number/cell)	Control		35.7% (26)	35.3% (11)	31.3% (8)
	Cpt		79.3% (54)*	68.4% (93)*	100% (36)*
	H <sub>2</sub> O <sub>2</sub>		49.9% (22)*	50.2% (49)*	33.6% (29)*

The data pertinent to the percentage of  $\gamma\text{H2AX}$  foci associated with replicating regions (after subtracting the control) were analyzed by the Student's test, the values that are statistically different from control (95% confidence limit) are marked with asterisk.

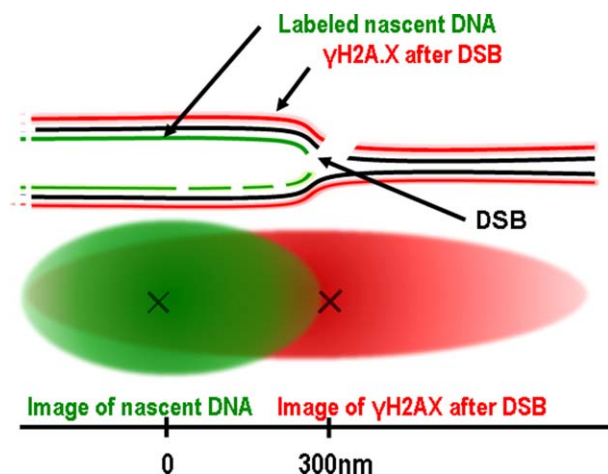


**Figure 6.** Schematic representation of regions of DNA replication, phosphorylation of histone H2AX, and the corresponding images. Even when the damage is inflicted in a region of DNA replication, the barycenters of images representing DNA replication and histone H2AX phosphorylation do not necessarily overlap. [Color figure can be viewed in the online issue which is available at [wileyonlinelibrary.com](http://wileyonlinelibrary.com).]

and (iv) moving the centers of fluorescently labeled regions of replication and histone phosphorylation apart during a chromatin relaxation (21) which might reach 100 nm in the case of the experimental protocol we used. Thus, we estimate “the critical distance” to be  $\sim 700$  nm for the early- and mid-S phase, and  $\sim 900$  nm for the late S-phase cells.

The accuracy of the estimate of the size of the “critical distance” is fairly limited. Thus, we investigated the influence of setting the value of the “critical distance” on the number of events that are consequently qualified as dependent or independent. The number of H2AX phosphorylation foci recognized as related to replication, plotted as a function of the selected size of the “critical distance,” is shown in Figure 7. As expected, this dependence is very weak in control cells, where intrinsic H2AX phosphorylation appears to be unrelated to replication. The dependence is very strong for Cpt-treated cells, because in this case a large proportion of  $\gamma$ H2AX foci are

located close to replication. In cells treated with  $H_2O_2$ , the dependence is less strong, because the majority of  $\gamma$ H2AX foci are seen at a large distance from replication. Conspicuously, the curves representing late S-phase in Cpt- and in  $H_2O_2$ -treated cells exhibit a change in slope at  $\sim 400$  and  $\sim 1000$  nm, respectively. These slope changes correspond to distances delineating the areas characterized by abundant and infrequent H2AX phosphorylation foci. As most Cpt-induced H2AX phosphorylation foci are close to replication, the curve bends near the value corresponding to a short distance, whereas in  $H_2O_2$ -treated cells this distance is larger.

#### Relationship Between $\gamma$ H2AX Foci Induced by Cpt or $H_2O_2$ and Replication

Based on the available knowledge, it was reasonable to expect that Cpt can damage DNA in replicating regions only, whereas  $H_2O_2$  might damage replicating as well as nonreplicating sections (5,6,8). Analysis of the 3D images of replication and histone phosphorylation should resolve the question whether the previously reported higher susceptibility of replicating versus nonreplicating cells to  $H_2O_2$ -induced damage arises from specific lesions induced in replicating DNA.

The early-, mid-, and late-S histograms representing distances from Cpt-induced phosphorylation foci to the nearest replication region show a similar tendency—a vast majority of phosphorylation sites are found close to replication (Fig. 4). As described above, late S-phase reveals the spatial relationship between the two events most clearly. According to the definition of the “critical distance” described above, in late S-phase all Cpt-induced phosphorylation foci are found to be adjacent to the replication regions present when Cpt exposure commenced (Fig. 4I), and all such replication regions are associated with the  $\gamma$ H2AX foci. Unexpectedly, in early and mid S-phase, some phosphorylation sites are detected at a distance greater than 700 nm from replication sites. This seems to contradict the notion that all Cpt-induced damage occurs only in replication forks, or suggests that the critical distance was set incorrectly, at too low a value. However, we note that the replication forks that terminated their movement shortly after addition of EdU or commenced replication just before cell fixation are likely to have incorporated only an

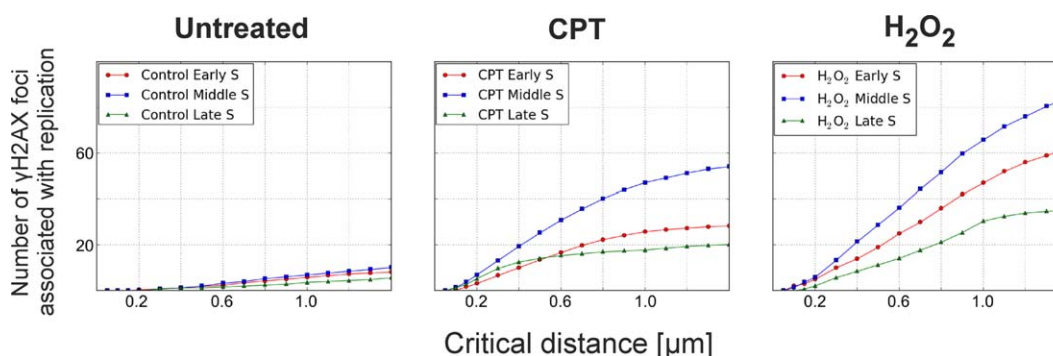


**Figure 7.** The influence of the value of the “critical distance” (see text for a definition) between the centers of regions representing DNA replication and H2AX histone phosphorylation on the number of events qualified as dependent (neighboring, i.e., replication regions with the adjacent histone H2AX phosphorylation focus) in untreated, and Cpt- and  $H_2O_2$ -treated cells. [Color figure can be viewed in the online issue which is available at [wileyonlinelibrary.com](http://wileyonlinelibrary.com).]

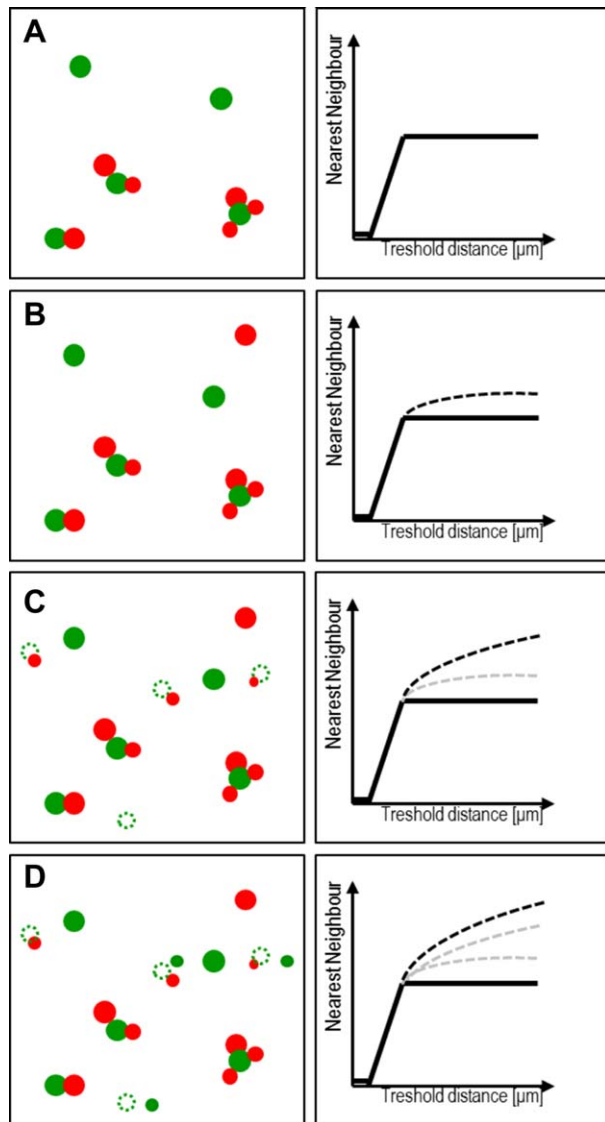


**Figure 8.** Schematic representation of various possible positions and labeling efficiencies of foci of type X (for example DNA replication) and type Y (for example histone H2AX phosphorylation). This illustrates the influence of the unlabeled foci on the shape of a curve depicting the number of independent events (as in Fig. 7). **A:** All foci are labeled, all Y cluster at X; **(B)** most Y cluster at X, but some X are not associated with Y; **(C)** as in (B) plus some X are poorly labeled so their association with Y is not detected; **(D)** as in (C) plus some new small foci X are created in response to clustering of Y at the previously existing X foci; the new foci are detectable. [Color figure can be viewed in the online issue which is available at [wileyonlinelibrary.com](http://wileyonlinelibrary.com).]

undetectable amount of the precursor, as explained in the scheme in Figure 8. In such cases, the replication that was a target of Cpt is not detected and the  $\gamma$ H2AX focus is incorrectly counted as replication-independent. There are also some replication foci detected in early S with no apparent association to  $\gamma$ H2AX (Fig. 4C and a scheme in Fig. 8). However, this sub-stage of S-phase is characterized by a large number of small replication foci. It is, therefore, possible that the

period of 30 min is not sufficient for Cpt (at the concentration we used) to bind (and induce damage) in all replication forks active in early S, or some replication foci are newly formed, as discussed below.

The same reasoning, which was described in the case of Cpt, can be applied to the analysis of images of cells exposed to  $H_2O_2$  (Fig. 5). In the case of  $H_2O_2$ -induced damage, the late S-phase is also the period that most accurately can reveal the spatial relationships between replication and damage. We have analyzed the 3D images and subtracted the histograms representing endogenous (intrinsic) phosphorylation in the same way as in the case of Cpt (Fig. 5B, E, H). The histograms representing distances between  $H_2O_2$ -induced  $\gamma$ H2AX foci and replication indicate that there are more H2AX phosphorylation sites in S-phase than in nonreplicating cells, consistent with the previous data obtained by LSC (5,6). However, only some  $\gamma$ H2AX foci were actually being induced in the replication areas. Thus, no clear preference for the induction of  $\gamma$ H2AX within the replicating regions was apparent (Fig. 5C, F, I). This observation is also consistent with the fact that  $\gamma$ H2AX foci are more frequent in nonreplicating  $H_2O_2$ -treated cells ( $\sim 83 \pm 31/\text{nucleus}$ ) than in nonreplicating untreated control ( $\sim 11 \pm 18/\text{nucleus}$ ), i.e., DNA damage signaling is strongly elevated following exposure to  $H_2O_2$  regardless of the phase of the cell cycle. These observations reinforce the conclusion that, although  $H_2O_2$ -induced  $\gamma$ H2AX foci are more frequent in S-phase than in G1, DNA damage signaling is generated principally outside of the replicating regions.

#### Activation of New DNA Replication Origins (ORI) in Cpt- and $H_2O_2$ -Treated Cells

It is conspicuous that in all stages of S-phase the total number of replication sites is greater in Cpt- and  $H_2O_2$ -treated cells than in untreated cells (Table 1). This observation appears to be in conflict with the fact that Cpt induces DSBs and halts replication, since a lower, rather than a higher number of detectable replication foci should be expected in cells challenged with this drug. The increased number of replication foci that we observed may actually reflect activation of new replication forks in response to stalling the already existing ones by Cpt. It is possible that the newly activated replication origins are active sufficiently long so as to incorporate a detectable amount of the precursor before being also stalled by Cpt. One can hypothesize that, despite the presence of Cpt, some new replication origins (ORI) are activated (as discussed in (22) and the references cited therein) at distances large enough to be detected by confocal microscopy. Notably, the increase of the number of replication sites is higher in the case of Cpt, which specifically attacks replication forks, but not as high in the case of  $H_2O_2$ , which exhibits only a limited tendency to damage replicating regions.

## DISCUSSION

### The Method—Advantages and Limitations

The method of quantitative analysis of spatial relationship between H2AX phosphorylation and DNA replication, which is introduced in this report, yields the expected results

in the case of Cpt-induced damage. The most suitable period for analysis is late S-phase. The nearest neighbor analysis of  $\gamma$ H2AX and replication sites indicate that a great majority or even all of the damage events induced by Cpt occur in the regions of replicating DNA, as would be expected (12,13,23). This result validates the method as a tool in quantitative assessment of spatial relationships between discrete cellular events.

The analysis of H<sub>2</sub>O<sub>2</sub>-induced DNA damage leads to a conclusion that, although the DDR is elevated in S-phase, the damage is not inflicted preferentially in replicating DNA. Combined with the Cpt data, this observation reinforces the notion that the method we describe can be applied to studies of spatial relationship between discrete cellular events. Moreover, the analysis of H<sub>2</sub>O<sub>2</sub>-induced DNA damage opens an interesting question about a possible mechanism that confers higher vulnerability of DNA to oxidative damage in S-phase. As mentioned, the data presented here and previously (5,6) indicate that whereas the incidence of DNA damage signaling induced by H<sub>2</sub>O<sub>2</sub>, as detected by  $\gamma$ H2AX foci, is higher in S-phase, it is not preferential to the DNA replicating sites revealed by the incorporated EdU. It is known that the primary product of oxidation of DNA bases is 8-oxo-7,8-dihydro-2'-deoxyguanosine (abbreviated 8-oxo-dG) (24) and it may be expected to be generated randomly in nuclear DNA. There is also evidence demonstrating that oxidative stress can induce signaling pathways and lead to induction of DNA replication fork stalling and general replication stress (25). Our data indeed show that only some  $\gamma$ H2AX sites induced in cells exposed to H<sub>2</sub>O<sub>2</sub> are associated with replication, while most of them are located at some distance from the replication sites that have incorporated EdU. This can occur if the DNA oxidation lesions, and resulting local changes in chromatin structure, are marked by histone H2AX phosphorylation, while replication forks are stalled at the same time by the signaling pathways. These two phenomena could result in the forks failing to reach the original 8-oxoG lesions during the course of the experiment. This is in contrast to DNA damage induced by Cpt, where DSBs are formed directly at the sites of the replication forks. However, the issue of higher incidence of H2AX foci in cells exposed to H<sub>2</sub>O<sub>2</sub> warrants further studies.

The currently described method of measuring spatial (3D) immediacy between the DNA replication sites and DNA damage sites ( $\gamma$ H2AX) induced by H<sub>2</sub>O<sub>2</sub> or by Cpt are also relevant to analysis of damage sites induced by endogenous oxidants related to constitutive DNA damage response (1–5) as well as to other DNA damaging agents that induce localized DNA damage response in forms of foci. These may be foci of ATM, p53 binding protein 1 (53BP1), Rad51 or Rad50.

The method of quantitative analysis of spatial relationship between discrete subnuclear events can be refined further. A better spatial resolution of foci in 3D images is required and may be possible with super-resolution 3D optical microscopy, like SIM, PALM, STORM, STED, etc. The algorithm for quantifying the probability of phosphorylation occurring accidentally within a replication region, as a function of the density of foci is reported in this article which accompanies this

report (26) (same issue). This improvement should assist in achieving a better assessment of a correlation between two types of events characterized by a high density, which is the case of replication and damage in early S-phase. It is worth noting that the approach we are describing here bridges the gap between LSC analysis of large numbers of cells and analysis of high spatial resolution deconvolved 3D confocal images of individual cells. Another example of an approach which makes it possible to exploit compatibility between a wide spectrum of cytometric methods, including flow cytometry, LSC, wide field, and confocal microscopy, has been described recently (27,28). This report also describes analysis of proximity between DNA replication and DNA foci, albeit using a different detection scheme (in situ proximity ligation assay).

The accuracy of detection of DNA damage signaling has limitations because of a relatively high and uneven background which seems always present in immunofluorescence detection of  $\gamma$ H2AX. This background may be a consequence of (i) the low level constitutive DNA damage induced by endogenous oxidants, (ii) autofluorescence, and (iii) nonspecific binding of the fluorochrome-tagged antibodies. The analysis would certainly benefit from better understanding or minimizing this background. It should also be noted that the intensity of  $\gamma$ H2AX fluorescence diminishes with time when its Ser139 becomes dephosphorylated in the course of DSBs repair (29).

Obviously, the method can only be applied to studies of nuclei with limited density of independent foci. Because at high density, foci cannot be resolved and counted only a certain range of damage levels can be analyzed accurately. A high-resolution, high-sensitivity microscope capable of detecting and imaging smaller foci in 3D space will expand the capabilities of this method to studies of a wider range of damage levels.

## CONCLUSIONS

1. The method of quantitative analysis of spatial relationship between discrete nuclear events described here is suitable for analysis of interdependencies between H2AX histone phosphorylation and DNA replication foci in cells subjected to treatments resulting in DSBs. This approach has a potential to be used for analysis of any other discrete cellular events detectable as a pattern of foci by 3D optical microscopy.
2. In cells subjected to H<sub>2</sub>O<sub>2</sub>, only a minor proportion of H2AX histone phosphorylation sites coincide with replicating areas. Thus, an increased level of histone phosphorylation which is seen in S-phase of cells subjected to oxidative stress induced by H<sub>2</sub>O<sub>2</sub> is not a direct consequence of DSBs inflicted on replicating DNA.
3. DNA damage and stalling of replicating forks caused by Cpt (or, to a lesser degree, H<sub>2</sub>O<sub>2</sub>) does not globally inhibit replication in the nucleus but appears to induce activation of new replication origins.

## ACKNOWLEDGMENTS

P.R. is a recipient of SET doctoral studentship from Jagiellonian University. A travel grant awarded by ISAC to P.R. to attend CYTO2012 is gratefully acknowledged.

## LITERATURE CITED

1. Tanaka T, Halicka HD, Huang X, Traganos F, Darzynkiewicz Z. Constitutive histone H2AX phosphorylation and ATM activation, the reporters of DNA damage by endogenous oxidants. *Cell Cycle* 2006;5:1940–1945.
2. Tanaka T, Kurose A, Halicka HD, Traganos F, Darzynkiewicz Z. 2-Deoxy-D-glucose reduces the level of constitutive activation of ATM and phosphorylation of histone H2AX. *Cell Cycle* 2006;5:878–882.
3. Tanaka T, Halicka HD, Traganos F, Darzynkiewicz Z. Phosphorylation of histone H2AX on Ser 139 and activation of ATM during oxidative burst in phorbol ester treated human leukocytes. *Cell Cycle* 2006;5:2671–2675.
4. Tanaka T, Kajstura M, Halicka HD, Traganos F, Darzynkiewicz Z. Constitutive histone H2AX phosphorylation and ATM activation are strongly amplified during mitogenic stimulation of lymphocytes. *Cell Prolif* 2007;40:1–13.
5. Zhao H, Tanaka T, Halicka HD, Traganos F, Zarebski M, Dobrucki J, Darzynkiewicz Z. Cytometric assessment of DNA damage by exogenous and endogenous oxidants reports aging-related processes. *Cytometry Part A* 2007;71A:905–914.
6. Zhao H, Dobrucki J, Rybak P, Traganos F, Halicka HD, Darzynkiewicz Z. Induction of DNA damage signaling by oxidative stress in relation to DNA replication as detected using “click chemistry”. *Cytometry Part A* 2011;79A:897–902.
7. Darzynkiewicz Z, Zhao H, Halicka HD, Li J. Cytometry of DNA replication and RNA synthesis: Historical perspective and recent advances based on “click chemistry”. *Cytometry Part A* 2011;79A:328–337.
8. Zhao H, Rybak P, Dobrucki J, Traganos F, Darzynkiewicz Z. Relationship of DNA damage signaling to DNA replication following treatment with DNA topoisomerase inhibitors camptothecin/topotecan, mitoxantrone, or etoposide. *Cytometry Part A* 2012;81A:45–51.
9. Darzynkiewicz Z, Zhao H, Halicka HD, Rybak P, Dobrucki J, Wlodkovic D. DNA damage signaling assessed in individual cells in relation to the cell cycle phase and induction of apoptosis. *Crit Rev Clin Lab Sci* 2012;49:199–217.
10. Huang X, Okafuji M, Traganos F, Luther E, Holden E, Darzynkiewicz Z. Assessment of histone H2AX phosphorylation induced by DNA topoisomerase I and II inhibitors topotecan and mitoxantrone and by DNA crosslinking agent cisplatin. *Cytometry Part A* 2004;58A:99–110.
11. Hsiang YH, Lihou MG, Liu LF. Arrest of replication forks by drug stabilized topoisomerase I-DNA cleavable complexes as a mechanism of cell killing by camptothecin. *Cancer Res* 1989;49:5077–5082.
12. Cleaver JE.  $\gamma$ H2AX: Biomarker of damage or functional participant in DNA repair “all that glitters is not gold!”. *Photochem Photobiol* 2011;87:1230–1239.
13. Sedelnikova OA, Rogakou EP, Panuytin IG, Bonner W. Quantitative detection of 125Iudr-induced DNA double-strand breaks with  $\gamma$ -H2AX antibody. *Radiat Res* 2002;158:486–492.
14. Salic A, Mitchison TJ. A chemical method for fast and sensitive detection of DNA synthesis in vivo. *Proc Natl Acad Sci USA* 2008;105:2415–2420.
15. Zhao H, Oczos J, Janowski P, Trembecka D, Dobrucki J, Darzynkiewicz Z, Wlodkovic D. Rationale for the real-time and dynamic cell death assays using propidium iodide. *Cytometry Part A* 2010;77:399–405.
16. Bolte S, Cordelières FP. A guided tour into subcellular colocalization analysis in light microscopy. *J Microsc* 2006;224:213–232.
17. Bernas T, Asem EK, Robinson JP, Rajwa B. Quadratic form: A robust metric for quantitative comparison of flow cytometric histograms. *Cytometry Part A* 2008;73A:715–726.
18. Leonhardt H, Rahn HP, Weinzierl P, Sporbert A, Cremer T, Zink D, Cardoso MC. Dynamics of DNA replication factories in living cells. *J Cell Biol* 2000;149:271–280.
19. Vilenchik MM, Knudson AG. Endogenous DNA double-strand breaks: Production, fidelity of repair, and induction of cancer. *Proc Natl Acad Sci USA* 2003;100:12871–12876.
20. Rogakou EP, Pilch DR, Orr AH, Ivanova VS, Bonner WM. DNA double-stranded breaks induce histone H2AX phosphorylation on serine 139. *J Biol Chem* 1998;273:5858–5868.
21. Halicka HD, Zhao H, Podhorecka M, Traganos F, Darzynkiewicz Z. Cytometric detection of chromatin relaxation, an early reporter of DNA damage response. *Cell Cycle* 2009;8:2233–2237.
22. Gilbert DM. Replication origin plasticity, Taylor-made: Inhibition vs. recruitment of origins under conditions of replication stress. *Chromosoma* 2007;116:341–347.
23. Koster DA, Palle K, Bot ES, Bjornsti MA, Dekker NH. Antitumour drugs impede DNA uncoiling by topoisomerase I. *Nature* 2007;448:213–217.
24. Aust AE, Eveleigh JF. Mechanisms of DNA oxidation. *Proc Soc Exp Biol Med* 1999;222:246–252.
25. Burhans WC, Weinberger M. DNA replication stress, genome instability and aging. *Nucleic Acid Res* 2007;35:7545–7556.
26. Bernas T, Berniak K, Rybak P, Zarebski M, Zhao H, Darzynkiewicz Z, Dobrucki JW. Analysis of spatial correlations between patterns of DNA damage response and DNA replication in nuclei of cells subjected to replication stress or oxidative damage. *Cytometry Part A* 2013; 83A: in press. DOI: 10.1002/cyto.a.22325.
27. Furia L, Pelicci PG, Faretta M. A computational platform for robotized fluorescence microscopy (I): High-content image-based cell-cycle analysis. *Cytometry Part A* 2013;83A:333–343.
28. Furia L, Pelicci PG, Faretta M. A computational platform for robotized fluorescence microscopy (II): DNA damage, replication, checkpoint activation, and cell cycle progression by high-content high-resolution multiparameter image-cytometry. *Cytometry Part A* 2013;83A:344–355.
29. Paris L, Cordelli E, Eleuteri P, Grollino MG, Pasquali E, Ranaldi R, Meschini R, Pacchierotti E. Kinetics of gamma-H2AX induction and removal in bone marrow and testicular cells of mice after X-ray irradiation. *Mutagenesis* 2011;26:563–572.